theory is based on simple physical considerations that large length scale polymer properties must provide universal laws embodying the long chainlike character of polymers. These laws are represented in terms of scaling laws and their generalization to the important regions of intermediate excluded volume where the power law exponents are no longer universal constants. A motivation is provided for the ϵ-expansion methods. The procedures for performing the ϵ-expansion calculations, evaluating the renormalization constants, and determining the generalized scaling functions are beyond the scope of this article. However, we summarize some of the major results for the excluded volume dependence of a variety of equilibrium and dynamic properties of polymers at infinite dilution in terms of the same variables employed to analyze experimental data. The agreement between theory and experiment is very good especially for the crossover regime which is inaccessible to previous theories. It will be of interest to extend these theoretical methods to more complicated polymer systems[50,51] where there are too many relevant parameters for simple scaling[13b] arguments to provide an adequate zeroth order description.

This work is supported, in part, by NSF Grant DMR83-18560 (polymers program) and is based primarily on the work with my students and research associates Y. Oono, A. Kholodenko, and J. Douglas, without whom this research would not have been possible.

(50) Miyaki, A.; Freed, K. F. *Macromolecules* **1983**, *16*, 1228; **1984**, *17*, 678.
(51) Freed, K. F. *J. Chem. Phys.* **1983**, *79*, 3121. Nemirovsky, A.; Freed, K. F., to be published.

Local Mode Overtone Spectra

M. S. CHILD

Theoretical Chemistry Department, University of Oxford, Oxford OX1 3TG, England

Received April 18, 1984 (Revised Manuscript Received October 5, 1984)

The concept of a normal mode plays an important part in vibrational theory whether for molecules, musical instruments, or engineering structures. In molecules certain vibrational modes are localized. A familiar example is a bond vibration with a frequency so disparate from others in the molecule that it is effectively uncoupled from other degrees of freedom, such as the ν_1 C–H stretching mode of $CHCl_3$. The success of infrared spectroscopy as an analytical tool depends on recognition of characteristic local bond or local group frequencies of this type. This Account deals with a more sophisticated form of localization that can develop in molecules for which the forms of coupled normal modes are determined by symmetry. The meaning of the term "local" has subtleties attached to it in this context, but there is no doubt that the concept has had signal success in the interpretation of multiquantum (overtone) absorption spectra, which are now becoming accessible by laser spectroscopy.[1,2]

In order to explain this new kind of localization it is convenient to start from a classical model. Imagine a molecule containing two equivalent bonds with a common frequency ω_0. Oscillations in one of them will be resonantly excited by vibrations in the other and energy will flow between them at a frequency ω_1 governed by the strength of interbond coupling. The ensuing motion may then be decomposed into two concerted normal mode motions[3] with frequencies $\omega_0 \pm \omega_1$. This normal mode picture depends however on the harmonic approximation—Namely that ω_0 and ω_1 are independent of energy. In a more realistic anharmonic model the individual bond frequencies will vary with energy, typically decreasing, for stretching vibrations, as the energy increases. This means that highly excited bonds will have a different natural frequency ω_0' from one that is unexcited. The coupling between them will therefore be effectively quenched if this anharmonic detuning is large and the interbond coupling is relatively weak. Classical studies on a realistic potential function confirm that one can observe a permanent imbalance between the two local bond excitation states of H_2O for example.[4] More detailed analysis of this classical situation may be found in papers by Lawton and Child,[5] Jaffé and Brumer,[6] and Sibert et al.[7] We note here two important observations. First, that the conditions of large anharmonicity and weak interbond coupling are most easily satisfied by the stretching of X–H bonds. Second, the two possible distributions of separate quanta in the two bonds gives rise to a twofold classical local mode degeneracy, with higher degeneracies if the number of equivalent bonds is increased.

The main purpose of this Account is to outline the quantum-mechanical analogue of this picture. One important change is that the quantum-mechanical states must of course carry the proper symmetry labels for the system. Thus the theory is developed in terms of symmetry adapted local mode states, given, in the case of two oscillations, by

Mark S. Child was born in England in 1937. He received his B.A. (1959) and Ph.D. (1962) from Cambridge University and did postdoctoral work at the University of California, Berkeley, in 1962–1963 with Professor D. R. Herschbach. After 3 years at Glasgow University, he moved to Oxford University, where he remains today. His research interests are classical and quantum mechanical theories of molecular collisions and spectroscopy.

(1) J. S. Wong and C. B. Moore in "Frontiers of Chemistry", K. J. Laidler, Ed., Pergamon., Oxford, 1982, p 353.
(2) M. E. Long, R. L. Swofford, and A. C. Albrecht, *Science (Washington D.C.)*, **191**, 183 (1976).
(3) See G. Herzberg, "Infra-red and Raman Spectra", Van Nostrand-Reinhold, New York, 1945.
(4) R. T. Lawton and M. S. Child, *Mol. Phys.*, **37**, 1799 (1979).
(5) R. T. Lawton and M. S. Child, *Mol. Phys.*, **44**, 709 (1981).
(6) C. Jaffé and P. Brumer, *J. Chem. Phys.*, **73**, 5646 (1980).
(7) E. L. Sibert, W. P. Reinhardt, and J. T. Hynes, *J. Chem. Phys.* **77**, 3583 (1982).

0001-4842/85/0118-0045$01.50/0 © 1985 American Chemical Society

$$|n,m^{\pm}\rangle = 2^{-1/2}(|n,m\rangle \pm |m,n\rangle)$$

where $|n,m\rangle$ denotes a state with n local quanta in the first oscillator and m in the second. Quantum-mechanical effects also give rise to an energy splitting that lifts the strict classical degeneracy, but decreases markedly with increasing energy. Notice the analogy here between the conventional picture of atomic spectroscopy—electronic motion, of course, being far from anharmonic. The 1s*n*s configuration of He for example corresponds to a local assignment of one electron to the 1s and the other to an *n*s state. The proper symmetrization gives rise to ^1S and ^3S terms that are split by the electrostatic interactions with a magnitude that decreases markedly with n.

The strongest local mode effects in molecules are observed in the above $|n,m^{\pm}\rangle$ states with $n = 0$ and m increasing. These include (i) the observation that successive $|0,m\rangle$ absorption band frequencies are well approximated by a single Morse oscillator expression;[8,9] (ii) the development of increasingly close local mode degeneracies;[10] (iii) predominant intensity in the $|0,0\rangle \rightarrow |0,n\rangle$ rather than $|0,0\rangle \rightarrow |1,n-1\rangle$ etc. absorption bands, indicative of the local excitation of a single mode;[11] and (iv) the insensitivity of X–H bandwidths and absorption frequencies to deuterium substitution, while the intensity varies in proportion to the number of unsubstituted X–H bonds.[12,13] It should also be noted that the widths of the bands are indicative of the rate of intramolecular transfer to the rest of the molecule. Thus the possibility of local excitation to high vibrational levels can provide a convenient means for the experimental study of this interesting process.[14,15]

Although the most strongly developed local mode effects are seen in the $|0,m\rangle$ excitation states, it is of interest to examine the character of other states and their energy dispositions. This not only helps complete the theoretical picture but also allows interpretation of the weaker bands in experimental overtone absorption spectra. It is here that knowledge of the relative strengths of bond anharmonicity and interbond coupling become very important. One can appreciate that strongly anharmonic and weakly coupled motions give rise to local mode effects, whereas weakly anharmonic, strongly coupled, motions are much more normal in character. These are, however, merely two extremes. There is a continuous scale between local and normal mode limits according to the ratio of bond anharmonicity to intermode coupling strength. It is shown below how one can construct a quantitative energy-level correlation diagram based on this idea, and how different molecules may be located on it. Earlier reviews of the salient features of the theory are available in the literature,[8,9,11] as is a fuller account of the present discussion.[16]

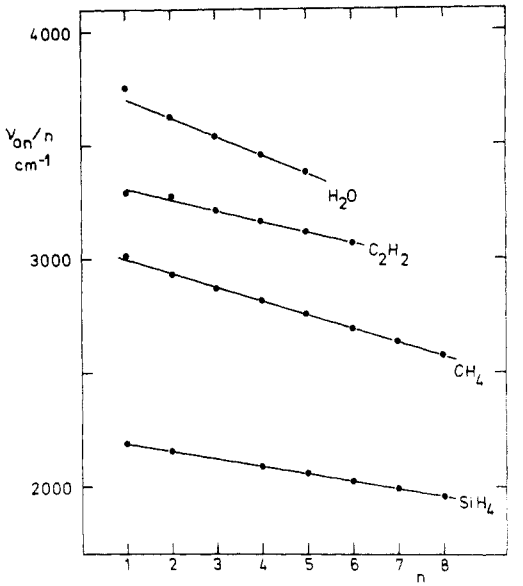

Figure 1. $\nu_{0,n}/n$ vs. n for the strongest overtone bands of H_2O, C_2H_2, CH_4, and SiH_4, based on data given by Child and Halonen[16] and Bernheim et al.[24]

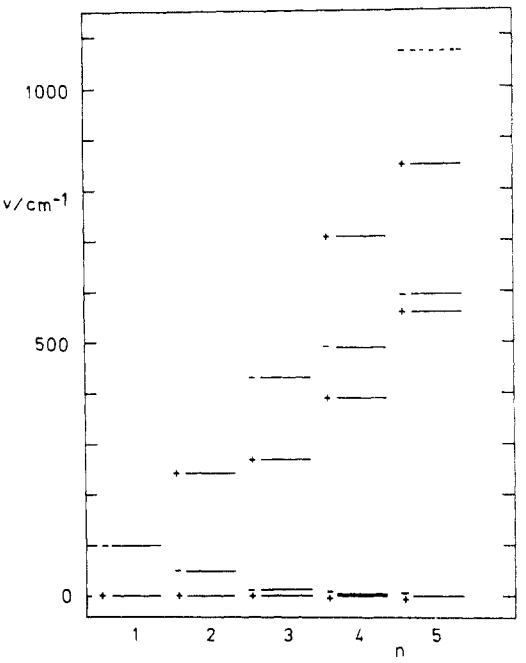

Figure 2. Splitting patterns of the observed stretching overtone manifolds of H_2O, as collected by Child and Lawton.[10] Signs ± indicate the symmetry with respect to rotation about the C_2 axis. The dashed level is calculated.[10]

Experimental Background

The development of local mode theory started from the observation[8,9] that the frequencies of the strongest overtone ($\Delta n \geq 2$) bands are consistent with a single mode oscillator model, with Morse energy levels[3]

$$E_n/hc = (n + \tfrac{1}{2})\omega - (n + \tfrac{1}{2})^2\omega x \qquad (1)$$

If so, the $0 \rightarrow n$ absorption frequency would become

$$\nu_{0,n} = n\omega - n(n+1)\omega x \qquad (2)$$

with the prediction that $(\nu_{0,n}/n)$ should be linear in n. Figure 2 shows that this is fully confirmed at high n values for a variety of molecules, the deviations for n

(8) B.R. Henry in "Vibrational Spectra and Structure", J. R. Durig, Ed., Elsevier, New York, 1981, Vol. 10.
(9) B. R. Henry, *Acc. Chem. Res.*, **10**, 207 (1977).
(10) See M. S. Child and R. T. Lawton, *Chem. Phys. Lett.* **87**, 217 (1982).
(11) M. L. Sage and J. Jortner, *Adv. Chem. Phys.*, **47**, 293 (1981).
(12) R. L.Swofford, M. E. Long, and A. C. Albrecht, *J. Chem. Phys.*, **65**, 179 (1976).
(13) R. L. Swofford, M. E. Long, M. S. Burberry, and A. C. Albrecht, *J. Chem. Phys.*, **66**, 664 (1977).
(14) R. G. Bray and M. J. Berry, *J. Chem. Phys.*, **71**, 4909 (1979).
(15) R. V. Reddy, D. F. Heller, and M. J. Berry, *J. Chem. Phys.* **76**, 2814 (1982).
(16) M. S. Child and L. Halonen, *Adv. Chem. Phys.* **57**, *1* (1984).

= 1–2 being attributable to normal mode mixing (see below).

Further support is provided by the variation of band intensity with isotope substitution. In benzene for example the frequencies of the dominant CH stretching overtone bands are invariant to isotopic substitution, but the integrated band intensities decrease proportionally with the number of hydrogen atoms from C_6H_6 to C_6D_6.[12,13] The suggestion is therefore that the local mode states of a molecule with N equivalent X–H bonds, are N-fold degenerate.

Closer analysis shows that while valid for some states this is an oversimplification. Figure 2 shows for example the observed vibrational term value for H_2O,[10] measured in each case from the lowest term value for the appropriate manifold, the term "manifold" being used to include all stretching states with a given total quantum number. It is evident that the lowest term values do approach a well-marked local mode degeneracy as n increases, the local mode splitting for n = 5 being only 0.4 cm^{-1}. The approach to an equivalent sixfold degeneracy is predicted[17] to be even more rapid in benzene, for which the 26 cm^{-1} spread of the CH stretching fundamentals[3] is much smaller than the 100 cm^{-1} splitting in H_2O. Figure 2 also shows a progressive decrease in the interval between third and fourth term values, but the general impression is one of irregularity. Thus a strict local mode description would be a gross oversimplification.

The final experimental observables to have attracted attention are the widths of different overtone peaks, and their possible relevance to the rate of intramolecular transfer from X–H modes to the rest of the molecule.[18] The observations include rotationally resolvable spectra for a variety of species including H_2O,[10] C_2H_2,[19,20] CH_4,[21,22] and SiH_4,[22–24] with individual line widths of 0.0067 cm^{-1} in the case of CH_4.[25] On the other hand, the gas-phase spectra of larger molecules show overtone band widths of the order of 50–100 cm^{-1}. The most famous example is benzene for which the band widths increase from ~30 cm^{-1} at n = 1 to a maximum of ~110 cm^{-1} at n = 5 and then decrease to ~56 cm^{-1} at n = 9.[15] The existence of such broad peaks is evidence that the CH mode cannot be truly local in the sense that it is decoupled from other modes in the molecule. In fact the observations in benzene have been plausibly interpreted by Sibert et al.[26] in terms of a specific Fermi resonance, induced by geometrically determined momentum transfer coupling between the CH vibrations and a combination of in-plane CCH wag and C–C stretching modes. The overall band widths for both C_6H_1 and C_6D_6 are well accounted for by coupling between the states $|n_{CH},0_N\rangle$ and $|(n-1)_{CH},2_N\rangle$ where N denotes the wagging and CC stretching modes, leaving further coupling to $|(n-2)_{CH},4_N\rangle$ and other background states to fill in a smooth band envelope. A nice feature of this explanation is that the variation of band widths arises from the anharmonic variation in the CH level separations. One finds in fact that the broadest band for C_6H_6 occurs for n = 5 for which the local CH level separation, 2526 cm^{-1}, is approximately twice the degeneracy weighted average frequency of 1283 cm^{-1} for the wagging and C–C stretching modes.

Coupled Local Anharmonic Oscillators

The central importance of competition between interbond coupling and bond anharmonicity may be illustrated by considering the model hamiltonian

$$H/hc = H_a^\circ/hc + H_b^\circ/hc + k_{ab}q_aq_b + g_{ab}P_aP_b \quad (3)$$

where q_ν and P_ν denote the coordinates and momenta for the two oscillators ν = a, b, and H_ν° is a local mode Morse oscillator hamiltonian with eigenstates $|n_\nu\rangle$

$$H_\nu^\circ|n_\nu\rangle = hc[(n_\nu + \tfrac{1}{2})\omega - (n_\nu + \tfrac{1}{2})^2\omega x]|n_\nu\rangle \quad (4)$$

In constructing the matrix of H within a local mode product basis $|n_a,n_b\rangle$ it is of vital importance to include the anharmonic term in ωx in eq 4, but it is sufficient for illustrative purposes to evaluate the matrix elements of q_ν and P_ν in the harmonic approximation; errors will be of order $(\omega x/\omega)$. Since both q_μ and P_μ carry selection rules $\Delta n_\nu = \pm 1$ a given state $|n_a,n_b\rangle$ will be coupled to others such as $|n_a \pm 1, n_b \mp 1\rangle$, which differ from it in energy by terms of order ωx, and to other states $|n_a + 1, n_b + 1\rangle$ and $|n_a - 1, n_b - 1\rangle$ which are separated from it by energy gaps of roughly 2ω. Since $\omega \gg \omega x$ the dominant coupling will be with the former pair. Detailed analysis[27–29] shows that the relevant nonzero matrix elements take the form

$$\langle n_a + 1, n_b - 1|H|n_a,n_b\rangle = \lambda\sqrt{(n_a + 1)n_b}$$

$$\langle n_a - 1, n_b + 1|H|n_a,n_b\rangle = \lambda\sqrt{n_a(n_b + 1)} \quad (5)$$

where, if second-order interactions nonresonant modes $q_\pm$ with frequencies ω_μ are taken into account[28]

$$\lambda = \alpha + \beta + \sum_\mu \left\{ \frac{(\alpha_\mu + \beta_\mu)^2}{\omega - \omega_\mu} - \frac{(\alpha_\mu - \beta_\mu)^2}{\omega + \omega_\mu} \right\} \quad (6)$$

the α and β type terms arise from coupling via the momentum and coordinate dependent coupling, respectively. Specific expressions for these parameters are given elsewhere.[28]

The coupling scheme implied by eq 4 and 5 is illustrated in Figure 3, from which it is apparent that in the case that $\omega x \gg \lambda$, the lowest pair of levels for each manifold will be split in first, second, and third order for $n_a + n_b$ = 1, 2, and 3, respectively. Equally the upper level pair for $n_a + n_b$ = 3 will be split in first order, etc. The model therefore accounts for the pattern of observed H_2O term values shown in Figure 2.

Local to Normal Mode Correlations

One can proceed beyond these qualitative considerations to obtain explicit expressions for the eigenvalues.

(17) L. Halonen, *Chem. Phys. Lett.*, **87**, 221 (1982).
(18) E. J. Heller and S. Mukamel, *J. Chem. Phys.*, **70**, 463 (1979).
(19) G. J. Scherer, K. K. Lehmann, and W. Klemperer, *J. Chem. Phys.*, **78**, 2517 (1983).
(20) G. J. Scherer, K. K. Lehmann, and W. Klemperer, *J. Chem. Phys.*, **79**, 1369 (1983).
(21) L. P. Giver, *J. Quant. Spectrosc. Radiat. Transfer*, **19**, 311 (1978).
(22) L. Halonen and M. S. Child, *Mol. Phys.* **46**, 239 (1982).
(23) J. Bardwell and G. Herzberg, *Astrophys. J.* **117**, 462 (1953).
(24) R. A. Bernheim, F. W. Lampe, J. F. O'Keefe, and J. R. Qualey III, *J. Chem. Phys.*, **80**, 5906 (1984).
(25) C. E. Kefter, C. P. Conner, and W. H. Smith, *Chem. Phys. Lett.* **104**, 475 (1984).
(26) E. L. Sibert, W. P. Reinhardt, and J. T. Hynes, *J. Chem. Phys.* **81**, 1115, 1135 (1984).
(27) I. A. Watson, B. R. Henry, and I. G. Ross, *Spectrochim. Acta, Part A*, **37A**, 857 (1981).
(28) M. S. Child and R. T. Lawton, *Discuss. Faraday Soc.*, **71**, 273 (1981).
(29) O. S. Mortensen, B. R. Henry, and M. A. Mohammadi, *J. Chem. Phys.*, **75**, 4800 (1981).

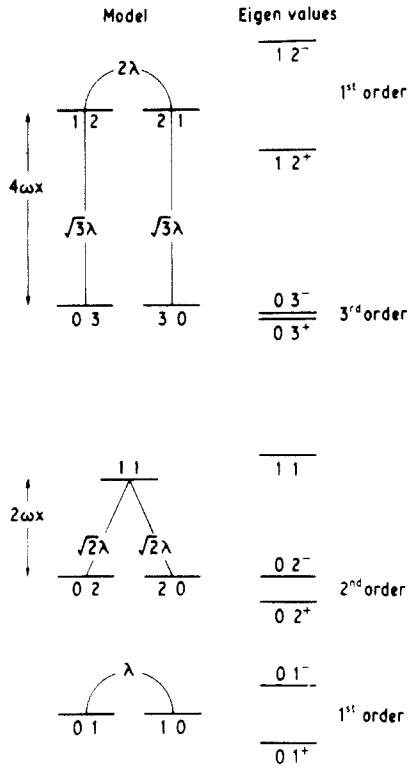

Figure 3. The anharmonic oscillator coupling scheme; zeroth order local mode labels $|n_a,n_b\rangle$ indicate individual bond excitations. $|n_a,n_b^{\pm}\rangle$ are symmetrized and antisymmetrized combinations. Taken from Child and Halonen[16] with permission of the publishers.

The calculation is simplified by adopting the symmetrized local mode basis with elements

$$|n,m^{\pm}\rangle = 2^{-1/2}(|n,m\rangle \pm |m,n\rangle) \text{ for } n < m$$

$$|n,n^{+}\rangle = |n,n\rangle \qquad (7)$$

where the first and second quantum numbers on the right-hand side refer to excitation of q_a and q_b, respectively. The resulting transformed matrices are given elsewhere.[28,29] It is convenient for presentation purposes to plot the splitting pattern for different manifolds by means of the reduced eigenvalues

$$\epsilon = [E - \bar{E}(n)]/[\lambda^2 + (\omega x)^2]^{1/2} \qquad (8)$$

where E denotes the eigenvalue in question and $\bar{E}(n)$ mean eigenvalue for the manifold (i.e., the set of states with given total quantum number (n). The variation of these reduced eigenvalues as a function of $(\lambda/\omega x)$ constitutes a correlation diagram between local ($|\lambda| \ll |\omega x|$) and normal ($|\lambda| \gg \omega x|$) limits.

Its form for two coupled oscillators is shown in Figure 4. The notation adopted is that the columns labeled "normal" give the conventional normal mode specifications, with ν_1 and ν_3 as the symmetric and antisymmetric modes, respectively. The central "local" labels, $|n,m\rangle$, specify the excitation states of the two local oscillators q_a and q_b. Finally solid and dashed lines denote respectively the variation of symmetric and antisymmetric reduced eigenvalues, ϵ, according to the ratio (λ/ω). The arctan scale is adopted to cover a wide range of $(\lambda/\omega x)$.

Notice that the eigenvalues are equally spaced in the limits $(\lambda/\omega x) \rightarrow \pm\infty$, in accordance with the familiar harmonic normal coordinate picture, with the ordering

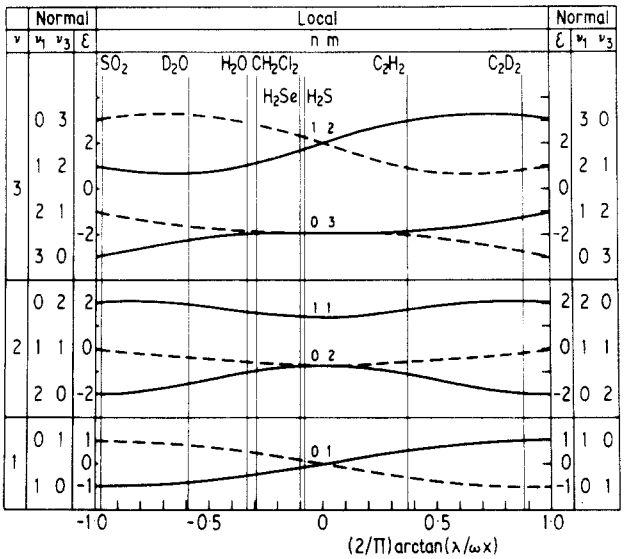

Figure 4. The local to normal mode correlation diagram for two coupled oscillators, indicating the positions of various molecules. Taken from Child and Halonen[16] with permission of the publishers.

of levels in the odd manifolds being dependent on the sign of $(\lambda/\omega x)$. The local limit, $(\lambda/\omega x) = 0$, on the other hand gives rise to two-fold $|n,m^{\pm}\rangle$ degeneracies which are split linearly, quadratically, and cubically in $(\lambda/\omega x)$ along the $|0,n^{\pm}\rangle$ sequence, in accordance with the coupling scheme in Figure 3.

The vertical lines show the location of different molecules on this diagram according to the λ and ωx parameters derived from their spectra;[28] ωx is available from the slope of $(\nu_{0,n}/n)$ vs. $(n + 1)$ as shown in Figure 1, and the fundamental splitting $(\nu_1 - \nu_3)$ may be shown to be equal to 2λ.[28,29] Equation 6 allows us to understand the relative postion of different molecules. For example the molecules in which the two modes are coupled via a central atom, give rise to negative λ values, this being the sign of the momentum transfer, α type, term in eq 6, which depends on the mass ratio of the peripheral to the central atom.[16] It is therefore not surprising that SO_2 is the most normal and H_2S and H_2Se the most local of this class of molecules, and that D_2O is more normal in behavior than H_2O. The potential coupling, β type, terms in eq 6 are of course also relevant to the position in the diagram, and detailed analysis[28] shows that these account in H_2O for roughly half the coupling strength λ. The occurrence of positive λ values for C_2H_2 and C_2D_2 is also readily understood in the light of eq 6 because there is no direct momentum coupling from one CH (or CD) bond to the other and very little direct potential coupling either[28,30] ($\beta \simeq \alpha = 0$). The dominant coupling is via the C–C mode (with coupling parameters α_μ and β_μ) which causes a positive contribution to λ in eq 6 if, as is the present case, $\omega > \omega_\mu$. The surprisingly large difference between near local behavior in C_2H_2 and near normal behavior in C_2D_2 is attributable not only to the change in mass ratio but more importantly to a much smaller resonance defect $\omega - \omega_\mu$ in the deuterated than in the hydrogenated molecule.[28,30]

Similar correlation diagrams have been worked out for AH_4,[22] $-AH_3$,[31] and XY_6[32] species; the results are

(30) L. Halonen, M. S. Child, and S. Carter, *Mol. Phys.*, **47**, 1097, (1982).

Table I
Observed[a,b] and Calculated[a] Term Values for CH_4 and SiH_4

			CH_4		SiH_4		
v	Γ	normal	ν_{obsd}/cm^{-1}	ν_{calcd}/cm^{-1}	ν_{obsd}/cm^{-1}	ν_{calcd}/cm^{-1}	local
1	A_1	ν_1	2916.47	2916.4	2186.87	2186.8	1000
	F_2	ν_3	3019.49	3021.0	2189.19	2189.0	
2	A_1	$2\nu_1$		5791.6	4308.38	4308.2	2000
	F_2	$\nu_1 + \nu_3$	5861	5856.4	4309.36	4309.3	
	F_2	$2\nu_3$	6004.65	6010.2	4378.5	4378.5	1100
3	F_2	$2\nu_1 + \nu_3$	8604	8612.5		6361.9	3000
	F_2	$\nu_1 + 2\nu_3$	8807	8807.8		6499.6	2100
	F_2	$3\nu_3$	8900	8909.5		6501.5	1110
	F_2	$3\nu_3$	9045.92	9041.7		6571.0	
4	F_2	$3\nu_1 + \nu_3$	11270	11262.5	8349.3	8347.0	4000
	F_2	$2\nu_1 + 2\nu_3$	11620[c]	11553.3		8554.3	3100
	F_2	$4\nu_3$	11885[c]	11907.2		8695.8	2110
5	F_2	$4\nu_1 + \nu_3$	13790	13796.4	10269	10264.3	5000
	F_2	$3\nu_1 + 2\nu_3$	14220	14206.9		10541.3	4100
	F_2	$5\nu_3$	14640[c]	14641.1		10751.0	3110
6	F_2	$5\nu_1 + \nu_3$	16160	16213.3	12121.2[b]	12113.7	6000
	F_2	$4\nu_1 + 2\nu_3$	16740	16745.1		12460.5	5100
7	F_2	$6\nu_1 + \nu_3$	18420	18513.5	13914.4[b]	13895.4	7000
	F_2	$5\nu_1 + 2\nu_3$	19120	19166.0		14312.0	6100
8	F_2	$7\nu_1 + \nu_3$	20600	20697.4	15625.4[b]	15609.3	8000
9	F_2	$8\nu_1 + \nu_3$	22660	22765.3	17266.6[b]	17255.4	9000

[a] See Halonen and Child[22] for references. [b] Bernheim et al.[24] [c] Tentative assignments made by qualitative intensity predictions.[16]

collected together with the appropriate coupling matrices in a more comprehensive review elsewhere.[16]

Potential Models and Variational Calculations

Early test calculations, based on a realistic but complicated potential surface for H_2O,[33] showed that a local mode Morse oscillator basis, as defined by eq 7, gave more rapid convergence than a conventional normal mode representation.[34,35] The calculated results were found to be in good agreement with experiment,[14] because the potential function[33] embodied a spectroscopically determined force field. One might however ask, in the light of sections 3 and 4, whether similar success could be obtained with a simpler potential function. How accurately for example could one describe the spectrum with a simple hamiltonian, as given in eq 3, if the simplifying approximations adopted in sections 3 and 4 were abandoned? The answer, for a variety of molecules, is very well indeed.

Table I gives comparisons between observed term values for CH_4 and SiH_4 and those calculated[16,22] from the four-bond analogue of eq 3 with two adjustable Morse parameters, ω and ωx, and one potential coupling parameter k_{ab}; the momentum coupling coefficient g_{ab} in eq 3 depends only on masses and geometrical factors.[16]

The table gives both normal mode and local mode assignments, the former for ease of comparison with the literature and the latter to emphasize the local characteristics of the situation. Notice that the observed, (presumably strongest) overtone bands are assigned in the normal mode picture to states $n\nu_1 + \nu_3$, which involve a $\Delta v = n$ transition in the optically inactive normal mode ν_1, combined with $\Delta v_3 = 1$. In the local picture, on the other hand, the same transitions more plausibly involve excitation by $(n + 1)$ quanta in a single bond mode.

The most striking feature of the table is however the predictive power of the three parameter model, which for CH_4, predicts the eight observations for $v = 1$–3 with a root mean square (rms) deviation of 5.4 cm^{-1} and the full 20 observations with an rms deviation of 45 cm^{-1}. Similarly, in the case of SiH_4, the rms deviation from the 11 observed term values is only 8 cm^{-1}. Comparable results have been reported for C_2H_2 and its isotopic variants,[30,36] a variety of XH_3D and XHD_3 species,[31] and SF_6, UF_6, and WF_6.[32]

The inclusion of SiH_4 in the table is of particular interest because the fundamental splitting $\nu_3 - \nu_1 \simeq 2.32$ cm^{-1}. Thus SiH_4 is the most extreme local mode molecule to have been studied in detail. SiD_4 on the other hand lies however roughly half way between local and normal limits in the appropriate coorelation diagram.[22] The reason for the difference is that the kinetic and potential contributions to the analogue of λ in eq 6 are of equal magnitude in SiH_4 but have opposite signs; hence $\lambda = (\nu_3 - \nu_1)/4 \simeq 0$. The kinetic (momentum transfer) term, α, is however relatively much more important in SiD_4, which accounts for the difference in behavior. A similar difference occurs between GeH_4 and GeD_4[22] but the available high overtone data are relatively limited.

Relevance of the Local Mode Pictures

The previous discussion has emphasized the local mode aspects of a particular type of motion—the stretching overtones of X–H bonds. Questions now arise as to the generality of this picture.

The low mass of the H atom is peculiarly significant in this context. First it gives rise to a typical stretching frequency $\omega \sim 3000$ cm^{-1} well separated from other modes, thereby minimizing coupling to other parts of the molecule, although the final part of section 2 shows that Fermi resonances may have significant effects. Secondly the anharmonicity parameter ωx, which is inversely proportional to reduced mass for a Morse oscillator,[37] is unusually large for XH bonds; $\omega x \sim$

(31) L. Halonen and M. S. Child, *J. Chem. Phys.*, **79**, 4355 (1983).
(32) L. Halonen and M. S. Child, *J. Chem. Phys.*, **79**, 559 (1983).
(33) K. S. Sorbie and J. N. Murrell, *Mol. Phys.*, **29**, 1387 (1975).
(34) R. T. Lawton and M. S. Child, *Mol. Phys.*, **40**, 773 (1980).
(35) H. S. Møller and O. S. Mortenen, *Chem. Phys. Lett.*, **66**, 539 (1979).
(36) L. Halonen, D. W. Noid, and M. S. Child, *J. Chem. Phys.*, **78**, 2803 (1983).

50–100 cm^{-1}, compared with 7.5 cm^{-1} for say SO_2.[28] Finally the inter-bond-coupling-strength term λ is dominated for stretching modes in most molecules, by momentum transfer terms dependent on the ratio of peripheral to central atom mass, giving rise to a value of $\lambda \simeq -100$ cm^{-1} in SO_2 compared with $\lambda \simeq -50$ cm^{-1} in H_2O.[28] The combination of the last two factors means that the ratio $|\lambda/\omega x|$ is much smaller (closer to the local mode limit) in H_2O than in SO_2. The arguments applying to the peculiar local mode advantages for X–H over other stretching modes apply even more strongly to bending and twisting modes which are if anything more harmonic than non X–H stretches.

One can also enquire into the effect of exciting other modes on the behavior of the X–H stretches. The experimental evidence in H_2O[28] and theoretical evidence of C_2H_2 and C_2D_2[30] is that such excitation has remarkably little effect on the spectrum, as shown for example by minimal changes in the local mode doublet splittings when H_2O is excited to the $v_2 = 1$ and $v_2 = 2$ levels of its bending vibration.[28] Thus, while local mode behavior is probably a specifically X–H stretching phenomenon, it is also a persistent one. Moreover these are the motions whose overtone states are most readily accessible by modern techniques,[1,2,12,13] because one requires only 5–6 quanta of the high X–H stretching frequency to reach the convenient tunable dye laser spectroscopic region. It is therefore a happy coincidence that the new theory has been developed for the very molecules most open to experimental investigation.

Concluding Remarks

Attention has been concentrated above on the use of local modes for spectroscopic assignment and interpretation—an essential first step towards understanding the nature of vibrationally excited molecular motions.

The kinetic implication of local mode states have also attracted widespread attention under the heading "intramolecular relaxation".[38] One knows that current theories of unimolecular dissociation assume free energy flow within the molecule,[39] on a picosecond time scale, as required for consistency with experimental results.[40] At very low energies on the other hand energy is locked into one particular normal or local mode; otherwise the use of quantum mechanical labels would be meaningless. At what energy and by what mechanism does the transition from low energy "regularity" to high energy "chaos" occur?

Classical studies have charted the relative phase space fractions occupied by normal, local, and chaotic states as a function of energy for simple systems.[5,41,42] The results for the stretching states for H_2O[5,41] suggest a significant onset of chaotic trajectories at the expense of local ones at roughly 30,000 cm^{-1}, well above the highest analyzed spectroscopic bands. The regularity of the known spectrum of H_2O is consistent with this theoretical prediction.

The situation is rather different for larger molecules, with much higher densities of states. Here the existence of a significantly localized mode which is optically coupled to the ground state provides a window for observation of the strength of coupling to other degrees of freedom. The width of the band is of particular significance in giving, via the uncertainty principle $\Delta E \Delta \tau \simeq h$, a measure of the time $\Delta \tau$ for intramolecular relaxation, if for example the band were coherently excited by a pulse short compared with $\Delta \tau$.[18] It still remains to be established however whether all or merely some other modes are excited by the relaxation. The Fermi-resonance theory cited above for the bandwidths in benzene[26] would require relaxation only into the C–C stretching and C–H wagging degrees of freedom for example.

These are only a few of the interesting problems for future investigation. Many fascinating questions remain to be answered.

(37) G. Herzberg, "Spectra of Diatomic Molecules", Van Nostrand, New York, 1950.
(38) See J. Jortner and B. Pallman, Eds., "Intramolecular Dynamics", Reidel, Dordrecht, The Netherlands, 1982.
(39) See J. Troe in "Physical Chemistry: an Advanced Treatise VIB", H. Eyring, D. Henderson, N. Jost, Eds., Academic Press, New York, 1975, Chapter 11.
(40) L. D. Spicer and B. S. Rabinowitch, *Annu. Rev. Phys. Chem.*, **21**, 349 (1970).
(41) J. T. Muckerman, D. N. Noid, and M. S. Child *J. Chem. Phys.*, **75**, 3981 (1983).
(42) T. Matsushita and T. Tevasaka, *Chem. Phys. Lett.*, **100**, 138 (1983).